



Full Length Article

Genetic inhibition of PPAR γ S112 phosphorylation reduces bone formation and stimulates marrow adipogenesis \star Chunxi Ge^a, Guisheng Zhao^a, BinBin Li^a, Yan Li^a, William P. Cawthorn^c, Ormond A. MacDougald^c, Renny T. Franceschi^{a,b,*}^a Periodontics & Oral Medicine University of Michigan School of Dentistry, University of Michigan School of Medicine, Ann Arbor, MI, United States^b Biological Chemistry, University of Michigan School of Medicine, Ann Arbor, MI, United States^c Molecular & Integrative Physiology, University of Michigan School of Medicine, Ann Arbor, MI, United States

ARTICLE INFO

Article history:

Received 31 July 2017

Revised 20 October 2017

Accepted 25 October 2017

Available online 26 October 2017

Keywords:

Genetic animal models

Transcription factors

Osteoblasts

Bone-fat interactions

ABSTRACT

A common feature of many skeletal diseases is the accumulation of marrow fat. A reciprocal relationship exists between osteogenesis and adipogenesis in bone marrow that is mediated by the relative activity of PPAR γ and RUNX2 transcription factors. The ERK/MAPK pathway is an important inducer of MSC differentiation to osteoblasts and an inhibitor of adipogenesis that functions by phosphorylating RUNX2 and PPAR γ . To begin to assess the importance of this regulation *in vivo*, we examined the consequences of blocking one arm of this pathway, PPAR γ S112 phosphorylation, by evaluating the bone phenotype of PPAR γ S112A mutant mice. This mutation prevents MAPK phosphorylation and inhibition of PPAR γ transcriptional activity. Both male and female PPAR γ S112A mice had decreased tibial and vertebral BV/TV and decreased trabecular bone relative to wild type littermates. These results were explained by a decrease in bone formation and osteoblast activity in the absence of changes in resorption. In contrast, marrow adipose tissue, adipocyte markers and serum adiponectin were all dramatically increased. Bone marrow stromal cells isolated from PPAR γ S112A mice had elevated PPAR γ and preferentially differentiated to adipocytes while total and phosphorylated RUNX2 and osteoblastogenesis were inhibited, indicating that the PPAR γ S112A mutation affects bone in a cell autonomous manner. Changes in osteoblast/adipocyte lineage allocation in MSC cultures were also seen where CFU-OBs were reduced with a parallel increase in CFU-AD. This study emphasizes the importance of PPAR γ phosphorylation in controlling bone mass and marrow adiposity and demonstrates how a regulatory mutation in PPAR γ previously associated with peripheral fat metabolism can have broader effects on bone homeostasis that may in turn affect whole body energy metabolism.

© 2017 Elsevier Inc. All rights reserved.

1. Introduction

In addition to its roles in mineral homeostasis, bone has important functions in energy metabolism. It directly or indirectly responds to major metabolic regulators including insulin, leptin and adiponectin and produces the hormone-like factor, osteocalcin. Bone is also a significant fat repository *via* marrow adipose tissue (MAT) (for reviews, see [1,2]). Although it is the least well-described fat store, MAT may have important functions in energy metabolism. MAT occupies approximately 70% of bone marrow volume in adult humans and in anorexic subjects can represent up to 30% of total body fat (for review, see [3]). MAT

volume increases in a number of skeletal diseases including osteoporosis and disuse osteopenia and there is a strong inverse relationship between bone mass and marrow adiposity [4–8]. However, the underlying mechanisms controlling MAT formation and related deficits in bone mass under different physiological and pathological conditions are poorly understood. In this communication, we describe a new pathway for controlling MAT and bone mass involving post-translational modification of PPAR γ .

In bone marrow, osteoblasts and adipocytes differentiate from a common mesenchymal progenitor [9–11]. This process is controlled by the relative activity of two key transcription factors, RUNX2 and PPAR γ , which are mutually antagonistic. Accordingly, mouse embryo fibroblasts (MEFs) from *Runx2*-null mice, which are unable to form osteoblasts, preferentially up-regulate PPAR γ and differentiate to adipocytes. Conversely, MEFs from *Pparg*-null animals fail to form adipocytes, but express high levels of RUNX2 and readily differentiate to osteoblasts. Reintroduction of RUNX2 into *Runx2*^{-/-} MEFs restores osteoblast differentiation and suppresses adipogenesis while re-

\star Supported by NIH Grant DE11723, NIDDK Grant P30 DK092926 Michigan Center for Diabetes Translational Research (RTF), DK092759, DK095705, DK62876 (OAM) and K12 DE023574 (Junior Faculty Training Award, CG).

* Corresponding author at: Department of Periodontics and Oral Medicine, University of Michigan School of Dentistry, 1011 N. University Ave, Ann Arbor, MI 48109-1078, United States.

E-mail address: rennyf@umich.edu (R.T. Franceschi).

expression of PPAR γ in *Pparg*^{-/-} cells restores adipocyte differentiation and suppresses osteoblastogenesis [12,13].

Major control of RUNX2 and PPAR γ activity is provided by ERK/MAPK-dependent phosphorylation, which is responsive to a range of environmental cues including mechanical loading, extracellular matrix (ECM) composition and stiffness, hormone, growth factor and morphogen stimulation [14–20]. Phosphorylation of RUNX2 at S301 and S319 stimulates transcriptional activity [21–23] while S112 phosphorylation of PPAR γ is inhibitory [24,25]. In a recent study, we showed that manipulation of RUNX2 and PPAR γ phosphorylation by exogenous overexpression of constitutively-active or dominant-negative forms of the MAPK intermediate, MEK1, could preferentially stimulate osteoblast or adipocyte differentiation, respectively, in mesenchymal cells. Furthermore, prevention of RUNX2 phosphorylation by S301A, S319A mutation inhibited its ability to stimulate osteoblastogenesis and suppress adipogenesis while S112A mutation in PPAR γ rendered it resistant to MAPK inhibition, leading to increased adipocyte differentiation and suppression of osteoblast formation [26].

Taken together, these studies suggest that the relative activity of RUNX2 and PPAR γ as determined by their phosphorylation state is able to control overall levels of bone and MAT formation. Here we examine aspects of this hypothesis related to PPAR γ phosphorylation *in vivo*. This was accomplished by examining the bone phenotype of mice harboring an S112A mutation in PPAR γ rendering it resistant to MAPK inhibition. Although the metabolic and peripheral fat phenotype of these animals was previously described, MAT and skeletal properties were not examined [27]. As will be shown, bone mass, bone formation and osteoblast differentiation in PPAR γ S112A mice are dramatically reduced while MAT and adipocyte differentiation are increased. These results are related to the relative phosphorylation state and activity of PPAR γ and RUNX2 and may explain the observed metabolic phenotype of these animals.

2. Material and methods

2.1. Animals

PPAR γ S112A mutant mice in a C57BL/6 genetic background [27] were derived from frozen sperm obtained from the Mutant Mouse Regional Resource Center (stock number: 031828-MU). Recovery of this strain by *in vitro* fertilization was performed at the University of Michigan Transgenic Model Core. PPAR γ S112A mutant mice were maintained by breeding with wild type C57BL/6 mice obtained from the Jackson Laboratory. All animal studies were approved by the University of Michigan Committee on the Use and Care of Animals (UCUCA) and conformed to all guidelines and regulations for the protection of animal subjects. Mice were maintained on a standard chow diet and housed in specific pathogen-free AAALAC-certified facilities. After genotyping, littermates were assigned to the experimental groups indicated. No genotype-related changes in animal survival were observed.

2.2. Micro-computed tomography (μ CT) analysis of bone

Tibiae and L3 vertebrae were embedded in 1% agarose and placed in a 19 mm diameter tube and scanned over the entire length of the tibiae using a microCT system (μ CT100 Scanco Medical, Bassersdorf, Switzerland). Scan settings were: voxel size 12 μ m, 70 kVp, 114 μ A, 0.5 mm AL filter, and 500 ms integration time. All scans were analyzed using fixed thresholds (180 for trabecular bone and 280 for cortical bone). Trabecular parameters were collected from 50 sections (8 μ m/section) under growth plates of proximal tibia and anterior end of L3 vertebrae. Cortical data were collected from 30 sections above trabecular bone of tibia and fibula junction.

2.3. MAT analysis

After microCT scanning and calculation of osseous parameters including total tissue volume of bones (TV), samples were decalcified with 10% ethylenediaminetetraacetic acid. After fixation with 10% neutral buffered formalin for 24 h, the samples were incubated with 1% osmium tetroxide at room temperature for 2 h to stain marrow fat. Osmium staining was measured by microCT [28]. The osmium-staining volume (OSM), which reflects fat volume, was then calculated and expressed as a fraction of total tissue volume (OSM/TV). Changes in OSM/TV are not necessarily related to marrow adipocyte numbers since adipocyte sizes may vary.

2.4. Histomorphometric analysis of bone formation and resorption

For dynamic bone histomorphometry, mice were intraperitoneally injected with 30 mg/kg calcein 9 days prior to sacrifice and then with 10 mg/kg Alizarin Red at 2 days prior to sacrifice. Tibia were harvested and embedded with methyl methacrylate. Six-micron sections were cut using a Leica SM2500 metallurgical cutting system. For the measurement of *in vivo* osteoclast activity, tibiae were harvested from 12 week old mice. TRAP staining was performed on histological sections using a Sigma Trap staining kit (387-A). The fluorescently-labeled and TRAP stained images were photographed using a Nikon 50i microscope. Histomorphometric parameters for double labels and osteoclast activity were assessed using an OsteoMeasurexp system (OsteoMetrics Inc., GA, USA).

2.5. Cell cultures and *in vitro* differentiation

Primary calvaria osteoblasts and bone marrow stromal cells (BMSCs) were isolated as previously described from 5 month-old male wild type and PPAR γ S112A mutant mice [29,30]. Osteoblast differentiation was induced by growth in α -MEM/10%FBS containing 50 μ g/ml ascorbic acid and 10 mM β -glycerophosphate. For adipogenesis, cells were grown for 2 days in alpha-MEM medium containing 10% FBS, insulin (5 μ g/ml), dexamethasone (1 μ M), IBMX (500 μ M) and troglitazone (5 μ M), followed by growth in medium containing troglitazone (5 μ M) for 9 days. For analysis of BMSC lineage allocation, marrow was plated at a density of 2.5×10^5 nucleated cells/cm² and fibroblast (CFU-F), osteoblast (CFU-OB) and adipocyte (CFU-AD) colony forming units were measured [31]. For *in vitro* osteoclast differentiation, bone marrow macrophages were isolated and treated with M-CSF and RANKL [32]. Visualization of mineralization, fat droplet accumulation and osteoclast formation was achieved using Alizarin Red, Oil Red O or TRAP staining, respectively. For measurement of osteoclast induction, cells were stained for TRAP (Sigma staining kit) or grown on BioCoat Osteologic dishes (BD Biosciences) for 3 days before measurement of pit formation. Cell images were taken using an inverted phase contrast microscope (Nikon D300).

2.6. ELISA and real time RT-PCR analysis of differentiation markers

Serum was collected from 5 month-old mice. The following serum markers were measured by ELISA: osteocalcin (Biomedical Tech Inc.); CTX-1 and TRAP (Ids, Inc.); Adiponectin and Leptin (Life Technology, Inc.). Total RNA was isolated from bones or tissue cultures using TRIzol reagent (Invitrogen). Reverse transcriptase reactions were conducted with 2 μ g of total RNA. TaqMan reverse transcriptase reagents and primers were obtained from Applied Biosystems. PCR was performed using an ABI Prism 7700 sequence detection system using Gapdh mRNA as an internal control.

2.7. Quantitation of total and phosphorylated RUNX2 and PPAR γ

Western blot analysis was conducted as previously described using total protein extracts from BMSC and calvarial cultures [33]. Blots were probed using the following antibodies: total RUNX2 (MBL, Woburn, MA), S319-P-RUNX2 [33], total PPAR γ and S112-P-PPAR γ (Millipore, Billerica, MA). Blots were analyzed on a ChemiDoc Touch imaging system (BioRad).

2.8. Statistical analysis

All statistical analyses were performed using SPSS 16.0 Software. Unless indicated otherwise, each reported value is the mean \pm S.D. of triplicate independent samples for *in vitro* cultures or at least 6 animals per group for *in vivo* studies. Statistical significance was assessed using a one-way analysis of variance.

3. Results

3.1. PPAR γ S112A mutant mice have reduced trabecular bone

To determine the *in vivo* significance of PPAR γ S112 phosphorylation in the skeleton, the bone phenotype of 3 and 5 month-old male homozygous PPAR γ S112A mice was compared with heterozygote and wild type littermates (Suppl. Fig. 1, Fig. 1). Micro-CT analysis of 3 month old homozygous PPAR γ S112A tibiae showed an approximately 31% reduction of trabecular bone volume with accompanying reductions in trabecular thickness and increased trabecular space (Suppl. Fig. 1A, C–E) without significantly reducing trabecular number (Suppl. Fig. 1F) or cortical bone volume (Suppl. Fig. 1B). In 5 month-old animals, results were even more dramatic with a 43% loss of trabecular bone (Fig. 1A, B) an accompanying reduction in trabecular thickness (Fig. 1C), but not number (Fig. 1E), and increased trabecular spacing (Fig. 1D). Although the reduction in BV/TV in heterozygotes was not statistically significant, effects of a single copy of the mutant PPAR γ allele did reach significance for certain parameters such as the reduction in trabecular thickness and levels of Runx2 and Ibsp mRNA extracted from bone. In contrast, cortical bone was not affected under any condition (Fig. 1F). Significant although somewhat smaller reductions in trabecular bone were also observed in tibiae from 5 month-old female mice (Suppl. Fig. 2) as well as L3 vertebrae from 5 month-old males (Suppl. Fig. 3).

3.2. Bone loss in PPAR γ S112A mutant mice is explained by reduced bone formation

To determine the basis for observed changes in bone mass in PPAR γ S112A mutant mice, bone formation and osteoclast activity were analyzed in 3 month-old males. Dynamic histomorphometric measurements were made using Calcein and Alizarin Red double labeling. As shown in Fig. 1G–I, mineral apposition and bone formation rates were significantly reduced in homozygous mutant mice (approx. 67% reduction vs. WT). This decrease was accompanied by a large reduction in osteoblast differentiation marker mRNAs extracted from whole bone (*Runx2*, *Ibsp* and *Bglap2*, Fig. 1J–L). Consistent with the observed decrease in its mRNA, serum BGLAP2 protein levels were also reduced in PPAR γ S112A mice (Fig. 1M).

In addition to functioning in adipose tissue, PPAR γ is expressed in osteoclasts where it can stimulate differentiation, particularly after rosiglitazone treatment. Consistent with this role, osteoclast-selective knockout of *Pparg* was reported to induce osteopetrosis [34]. It is, therefore, possible that some of the bone loss observed in PPAR γ S112A mice is explained by increased osteoclastogenesis induced by the more active phosphorylation-deficient PPAR γ in these animals. To address this issue, we examined osteoclasts in wild type and PPAR γ S112A mutant mice (Suppl. Fig. 4). Histological sections of tibia from 3 month-old males were stained for tartrate-resistant acid phosphatase (TRAP)

(Suppl. Fig. 4A) and osteoclast parameters were determined. No significant differences in osteoclast surface, osteoclast number or osteoclast number/osteoclast surface were observed between WT, heterozygotic or homozygotic PPAR γ S112A mutant mice (Suppl. Fig. 4B–D). Consistent with these results, serum ELISA analysis failed to detect any differences in circulating levels of the osteoclast markers, TRAP and C-terminal telopeptide of Type I collagen (CTX-I, Suppl. Fig. 4E, F).

To examine possible effects of the PPAR γ S112A mutation on osteoclast differentiation *in vitro*, whole bone marrow macrophages were isolated from 12-week-old mice. Osteoclast differentiation was induced by treatment with exogenous M-CSF and RANKL. The number of induced macrophage clones, TRAP positive multinucleated cells and resorption pits formed were similar between WT and PPAR γ S112A mice (Suppl. Fig. 4G–K). Lastly, no differences were noted between WT and mutant cultures when the osteoclast differentiation marker mRNAs, *Nfatc1* and *Catk* were measured (Suppl. Fig. 4L, M).

Taken together, these results show that PPAR γ S112A mutant mice of both sexes have reductions in trabecular bone that are associated with reduced bone formation and osteoblast activity in the absence of changes in osteoclastic resorption.

3.3. PPAR-S112A mice have increased marrow adipose tissue

Previous characterization of the peripheral fat phenotype of PPAR γ S112A mice failed to detect increases in total white (WAT) or brown adipose tissue (BAT). However, because adipocyte size was reduced, it was determined that the total number of adipocytes was increased [27]. This is consistent with the known ability of the PPAR γ S112A mutation to increase transcriptional activity and adipocyte differentiation in mouse embryo fibroblasts cultured from these mice. However, this study did not examine MAT. Changes in marrow fat are of particular interest in view of the recent report that MAT may regulate whole body metabolism by modulating circulating adiponectin [5]. Analysis of MAT in 5 month-old males using osmium staining and μ CT imaging revealed dramatic increases in MAT in proximal tibiae of heterozygotic (1.4-fold increase vs. wild type) and, to a greater extent, homozygotic PPAR γ S112A mice (3.3-fold increase vs. wild type, Fig. 2). These changes were also apparent in histological sections from the same tibial region (Suppl. Fig. 4A). Consistent with the observed increases in MAT, large increases were also observed in adipocyte differentiation marker mRNAs (*Pparg*, *Cebpa*, *Fabp4* and *Adipoq*) in whole bone extracts from heterozygotic and homozygotic PPAR γ S112A mice (Fig. 2E–H). In agreement with a previous report [27], serum adiponectin protein levels also increased in heterozygous and homozygous PPAR γ S112A mice while leptin levels decreased (Fig. 3I, J). MAT in the distal tibiae of heterozygous and homozygous PPAR γ S112A mice was also increased 1.6 and 2-fold, respectively versus wild type (Suppl. Fig. 5).

3.4. Defective osteoblast differentiation and increased adipogenesis in BMSCs from PPAR γ S112A mice

The skeletal phenotype of PPAR γ S112A mice could be explained either by systemic effects of the mutation on bone homeostasis or direct actions on bone cells. Two approaches were taken to determine if the PPAR γ S112A mutation affects bone cells in a cell autonomous manner. In the first, BMSCs (adherent cells isolated from tibial marrow that are known to contain MSCs) were isolated from 12 week-old homozygous PPAR γ S112A mice or wild type littermates and grown in osteoblast or adipocyte differentiation conditions. Cells from PPAR γ S112A mice showed a severe defect in osteoblast differentiation with mineralization and levels of osteoblast marker mRNAs (*Runx2*, *Bglap2* and *Ibsp*) all being dramatically reduced (Fig. 3A–D). In contrast, adipogenesis as measured by Oil red O staining of lipid droplets and levels of adipocyte marker mRNAs (*Pparg*, *Cebpa*, *Adipoq* and *Fabp4*) clearly increased (Fig. 3E–I).

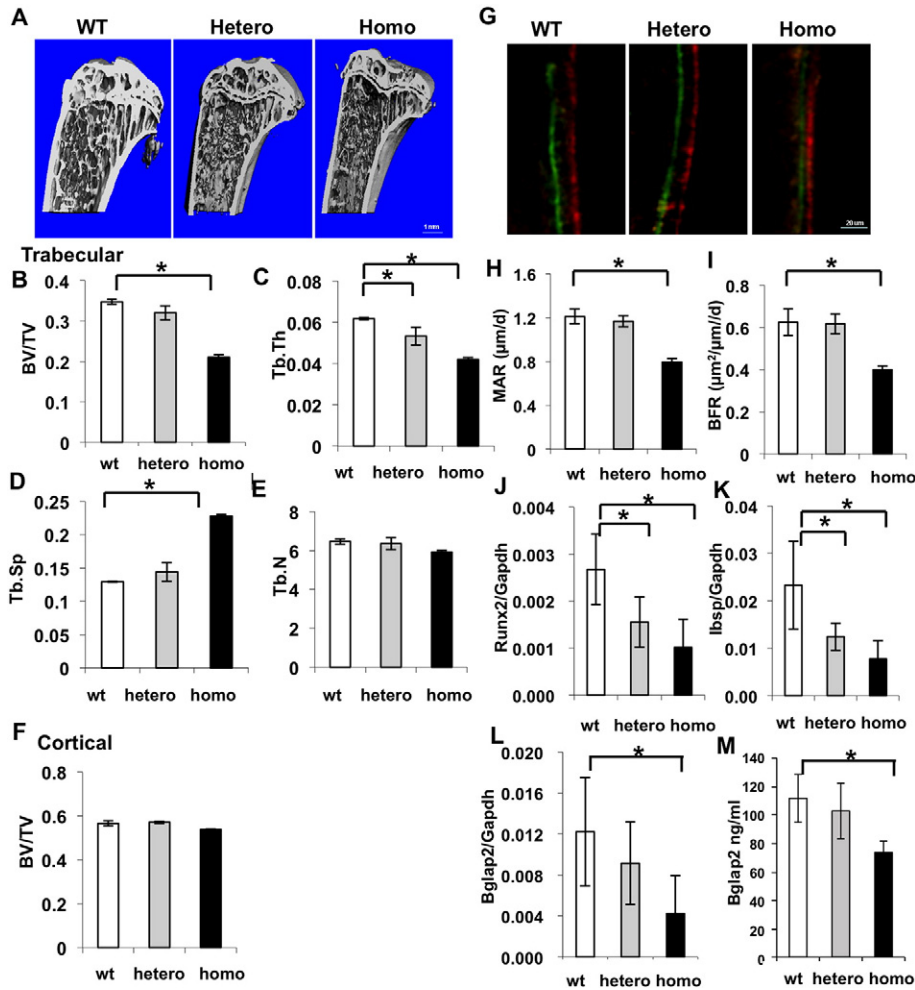


Fig. 1. PPAR γ -S112A mice have reduced trabecular bone. (A–E) MicroCT analysis. Tibias were isolated from 5 month-old wild type (WT), heterozygous (Hetero) and homozygous (Homo) PPAR-S112A male mice and bone parameters were measured. (A) Micro-CT images of proximal tibia. (B–E) Trabecular bone parameters. (B) Bone volume/tissue volume (BV/TV), (C) trabecular thickness (Tb.Th, μm), (D) trabecular spacing (Tb.Sp, μm), (E) trabecular number (Tb.N); (F) cortical bone volume/tissue volume (BV/TV). (G–I) Dynamic histomorphometry. Twelve week-old mice were injected with calcein and alizarin red and dynamic histomorphometric parameters were determined as described in the [Materials and methods](#) section. (G) Representative images of fluorescently labeled trabecular bone. (H) Mineral apposition rate (MAR) and (I) bone formation rate (BFR). (J–L) Osteoblast marker mRNAs. (J) *Runx2*, (K) *Ibsp* and (L) *Bglap2*. (M) Serum *Bglap2* levels. (* $p < 0.01$, $n = 6$ between groups designated with horizontal brackets).

A second series of studies examined possible changes in lineage allocation of MSCs within the BMSC population using clonal analysis. Equal numbers of nucleated cells from WT and PPAR γ S112A mouse marrow were plated at clonal density and ability to form fibroblast (CFU-F), osteoblast (CFU-OB) and adipocyte (CFU-AD) colony forming units was measured (Fig. 3J). The ability of MSCs to form fibroblast-like colonies was not significantly different between cells from PPAR γ S112A and WT animals. However, the phosphorylation site mutation severely restricted the ability of cells to form CFU-OB (approx. 40% inhibition) while simultaneously increasing CFU-AD (75% increase). Therefore, presence of a phosphorylation deficient mutant PPAR γ severely restricts the ability of BMSCs to form osteoblasts and this inhibition may be related to a defect in MSC lineage allocation resulting in increased adipogenesis and MAT.

3.5. Preferential suppression of RUNX2 and RUNX2 phosphorylation in BMSCs from PPAR γ S112A mice

Because both RUNX2 and PPAR γ are regulated by MAPK-dependent phosphorylation, we examined effects the PPAR γ S112A mutation on total and phosphorylated RUNX2 (S319-P) and PPAR γ (S112-P) protein levels during osteoblast and adipocyte differentiation of BMSCs using

the same conditions described in Fig. 3. Total RUNX2 protein levels from both WT and mutant mice gradually increased during growth in osteogenic media, but levels were approximately 25–30% lower in BMSCs from PPAR γ S112A mice (Fig. 4A,B). More dramatic effects of the PPAR γ mutation were seen when levels of phosphorylated RUNX2 were examined. Although the P-RUNX2/total RUNX2 ratio increased with time in both WT and mutant cells, phosphorylation was strongly suppressed in the PPAR γ mutant (up to 55% inhibition at 3 weeks). This result is consistent with the observed inhibition of osteoblast differentiation in cells from PPAR γ S112A mice shown in Fig. 3.

Conversely, when WT BMSCs were grown under adipogenic conditions, PPAR γ -S112 phosphorylation and the P-PPAR γ /total PPAR γ ratio rapidly declined (Fig. 4C, D). Consistent with the increased adipogenic activity of PPAR γ S112A mutant cells, the differentiation-dependent increase in total PPAR γ protein levels was greater in BMSCs from PPAR γ S112A mice when compared with WT controls.

3.6. Defective osteoblast differentiation and paradoxical adipogenesis in calvarial cultures from PPAR γ S112A mice

As shown in micro-CT images of skulls (Fig. 5M), PPAR γ S112A mutant mice had hypomineralized fontanelles and modest changes in skull

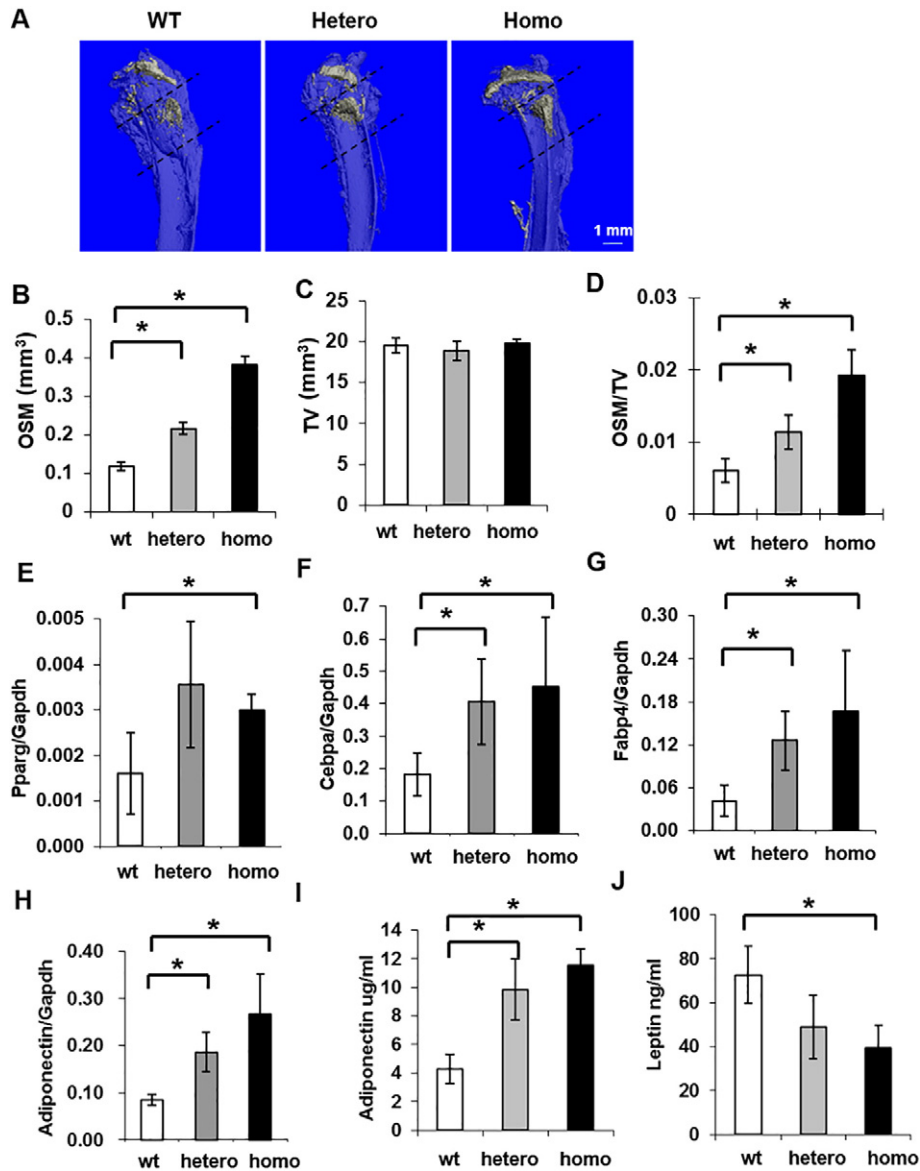


Fig. 2. PPAR γ -S112A mice have increased marrow adipose tissue in proximal tibiae. Analysis used the same bone samples as in Fig. 1. (A) Micro-CT images of demineralized proximal tibiae from wild type, heterozygous and homozygous PPAR-S112A female mice after osmium staining. (B–D) Calculation of total osmium volume (OSM), total tissue volume (TV) and osmium volume/total tissue volume (OSM/TV). Analysis was restricted to the volume between the dashed lines indicated. (E–H) Whole bone adipocyte marker mRNA levels: *Pparg* (E), *Cebpa* (F), *Fabp4* (G) and *Adipoq* (H). (I, J) Detection of serum adipocyte marker proteins by ELISA: adiponectin (I) and leptin (J). (* $p < 0.01$, $n = 6$).

morphology in addition to the above described changes in long bone development. To determine if this reduced mineralization was related to changes in cell differentiation, calvarial osteoblasts were isolated and grown under osteogenic and adipogenic conditions. Consistent with *in vivo* results, cells from homozygous PPAR γ S112A mice exhibited defects in osteoblast differentiation as measured by mineralization after 2 weeks in osteogenic medium (Fig. 5A) and in the time course of osteoblast marker mRNA expression (Fig. 5B–D). Interestingly, even though cells were grown in osteogenic medium, we observed spontaneous accumulation of fat droplets in PPAR γ S112A cells (Fig. 5E) as well as elevated levels of adipocyte differentiation markers that persisted throughout the differentiation time course (Fig. 5F–H). Differences between wild type and PPAR γ S112A cells were even greater when cells were grown in adipogenic medium (Fig. 5I–L). Consistent with the known osteoblast enrichment in calvaria-derived cells, very little oil red O staining was seen in wild type cells and this was accompanied by very weak expression of adipocyte marker mRNAs. In contrast, robust adipocyte differentiation was seen in cells from PPAR S112A mice.

4. Discussion

MAT has recently become the focus of renewed research interest both because of its possible relationship to skeletal disease and role in systemic metabolism [3]. The molecular signals regulating MAT expansion and contraction and its relationship to bone mass are unknown. On the basis of cell culture studies, we hypothesized that MAPK-dependent phosphorylation of PPAR γ and RUNX2 provides an important mechanism for regulating bone or MAT formation and that this is accomplished by controlling the differentiation of marrow MSCs to adipocytes or osteoblasts [26]. Specifically, activation of MAPK in mesenchymal cells was shown to stimulate phosphorylation of PPAR γ and RUNX2 leading to reduced adipocyte-specific transcription and differentiation and increased RUNX2 activity and osteoblastogenesis. The phosphorylation state of RUNX2 and PPAR γ controlled their ability to both stimulate their respective target genes as well as repress each other's transcriptional activity. Thus, wild type RUNX2 or, to a greater extent, RUNX2 containing phosphomimetic serine to glutamate

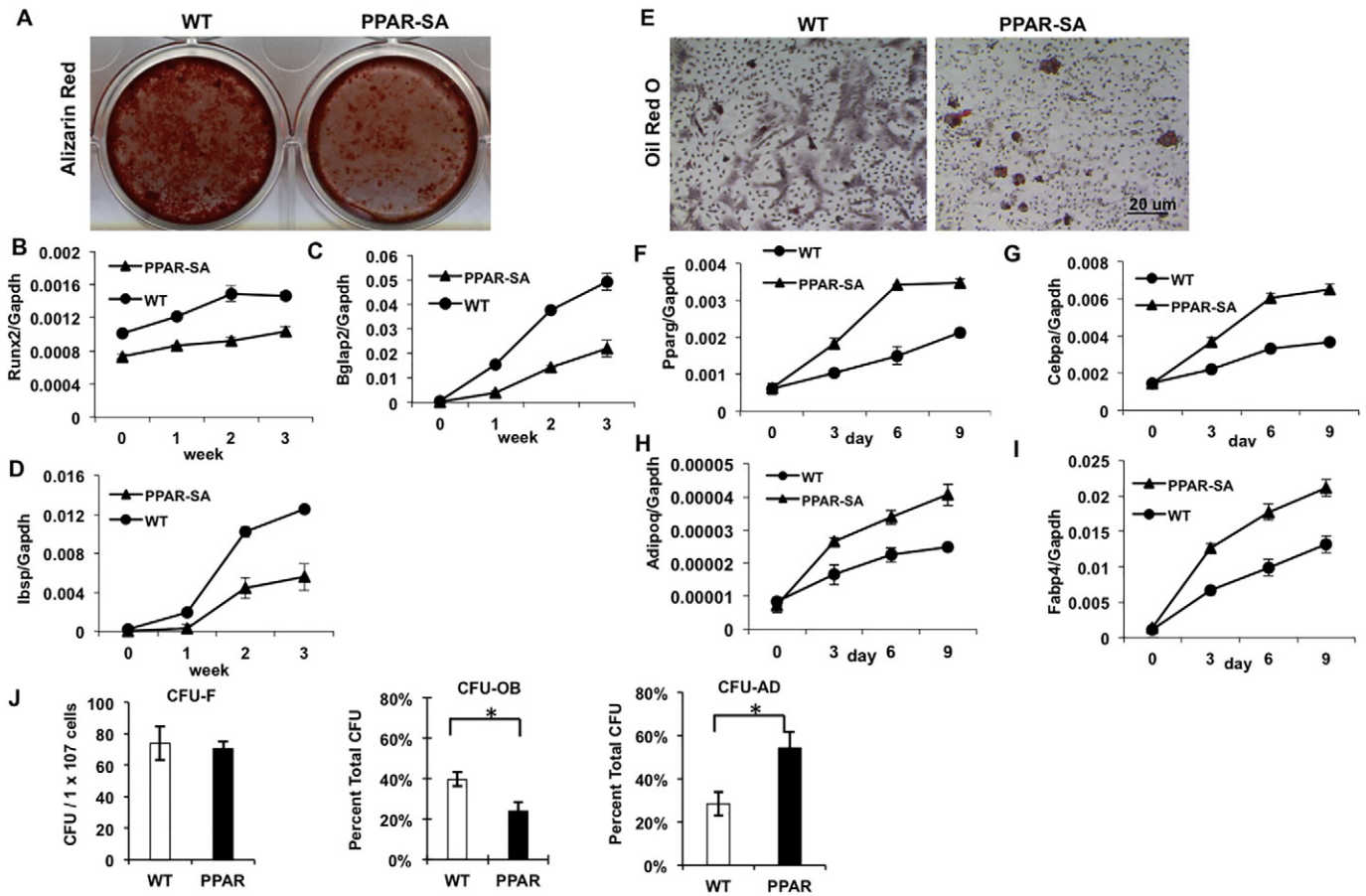


Fig. 3. Increased adipocyte differentiation and decrease osteoblast differentiation in BMSCs from PPAR γ -S112A mice, relationship to MSC lineage allocation. BMSCs were isolated from 5 month-old wild type and homozygous male PPAR γ S112A mice and grown in osteogenic (A–D) or adipogenic conditions (E–I). (A) Mineralization. Cells were stained with Alizarin red after 3 weeks in culture. (B–D) Osteoblast differentiation marker mRNAs. (B) *Runx2*, (C) *Bglap2* and (D) *Ibsp*. (E) Lipid droplet accumulation. Cells were stained with Oil red O after 9 days in culture. (F–I) Adipocyte differentiation marker mRNAs. (F) *Pparg*, (G) *Cebpa*, (H) *Adipoq* and (I) *Fabp4*. (J) Colony formation assay. BMSC were plated at clonal density and assayed for ability to form fibroblast-like colonies (CFU-F), osteoblast colonies (CFU-OB) and adipocyte colonies (CFU-AD).

mutations strongly suppressed PPAR γ expression and adipogenesis while a non-phosphorylated RUNX2 mutant had much less activity. Similarly, wild type PPAR γ or, to a greater extent, a non-phosphorylated PPAR γ mutant that could not be inhibited by MAPK were potent inhibitors of RUNX2 expression and osteoblastogenesis while WT or a phosphomimetic PPAR γ mutant were much less active.

The availability of PPAR γ S112A mice provided an opportunity to test portions of our hypothesis *in vivo* by determining whether interference with PPAR γ phosphorylation could inhibit RUNX2 activity, bone formation and increase MAT as was seen in cell culture. Because PPAR γ cannot be suppressed by phosphorylation in these animals, its adipogenic activity remains unchecked [27]. Consistent with our model, PPAR γ S112A mice have clear deficits in tibial and vertebral trabecular bone and increased MAT in proximal and distal tibiae as well as reduced calvarial mineralization. The decreased bone mass was explained by a selective reduction in osteoblast activity and bone formation rate *in vivo* and inhibition of BMSC osteoblast differentiation and MSC lineage allocation to osteoblasts together with concomitant increases in adipocyte formation (Fig. 3). Consistent with these changes, total and to a greater extent phosphorylated RUNX2 levels were suppressed in BMSCs from PPAR γ S112A mice grown in osteogenic medium (Fig. 4). The observed reduction in total RUNX2 is consistent with our previous study showing that the phosphorylation-resistant PPAR γ mutant can inhibit RUNX2 expression in mesenchymal cell cultures [26]. However, it does not explain why the ratio of P-RUNX2/Total RUNX2 was also reduced. One possibility is that the presence of the mutant PPAR γ may restrict access of RUNX2 to P-ERK. As shown in Fig. 5, PPAR γ S112A levels remain elevated even during osteoblast

differentiation, likely because the mutant protein cannot be inactivated by phosphorylation. The accumulated PPAR γ may sequester P-ERK away from RUNX2, thereby reducing phosphorylation.

Further support for the importance of RUNX2 and PPAR γ phosphorylation in the control of bone and MAT comes from our recent study on the phosphoprotein phosphatase, PP5 [35]. This molecule has the unique ability to dephosphorylate both RUNX2-S319-P and PPAR γ -S112-P leading to suppression of RUNX2 transcriptional activity and stimulation of PPAR γ . Consistent with these actions, mice deficient in PP5 have a phenotype that is the opposite of PPAR γ S112A mice with increased bone mass, increased RUNX2 and PPAR γ phosphorylation, reduced MAT and preferential MSC lineage allocation to osteoblasts. Interestingly, PP5-deficient mice are also resistant to the negative effects of the PPAR γ agonist, rosiglitazone, on bone mass.

Although previous studies indicated that osteoclast-selective knock-out of PPAR γ is able to induce osteopetrosis [34], we found no evidence that osteoclast activity was elevated in PPAR γ S112A mice or in marrow cultures from these animals. Consistent with this result, the increased bone mass previously observed in heterozygous PPAR γ -null mice was also attributed primarily to increased osteoblast activity and bone formation rather than a reduction in osteoclast formation [12]. Our results suggest either that PPAR γ phosphorylation is not a significant regulatory mechanism in osteoclasts or that the magnitude of its effects are insignificant compared with the more dramatic effects of mutant PPAR γ on osteoblast activity.

Because a global knock-in strategy was used to generate PPAR γ S112A mice, the possibility that changes in bone and MAT are indirectly mediated by peripheral tissues rather than reflecting direct effects of the

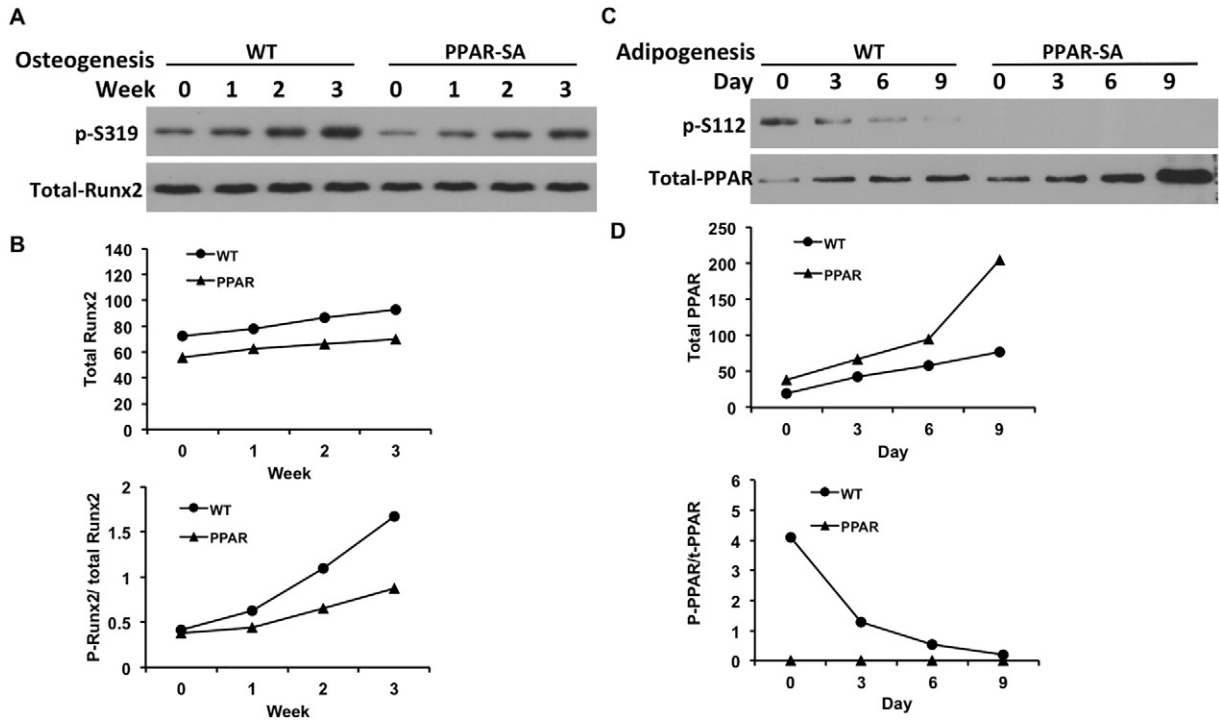


Fig. 4. Reduction in RUNX2 phosphorylation in BMSCs from PPAR γ -S112A mice. BMSC from WT or PPAR γ -S112A were grown in osteogenic (A, B) or adipogenic medium (C, D) as in Fig. 3 A–I. Cell extracts were prepared at the indicated times for measurement of total and phosphorylated RUNX2 (p-S319) or total and phosphorylated PPAR γ (p-S112). (B, D) Densitometric scans of Western blots and calculated P-RUNX2/total RUNX2 and P-PPAR γ /total PPAR γ ratios.

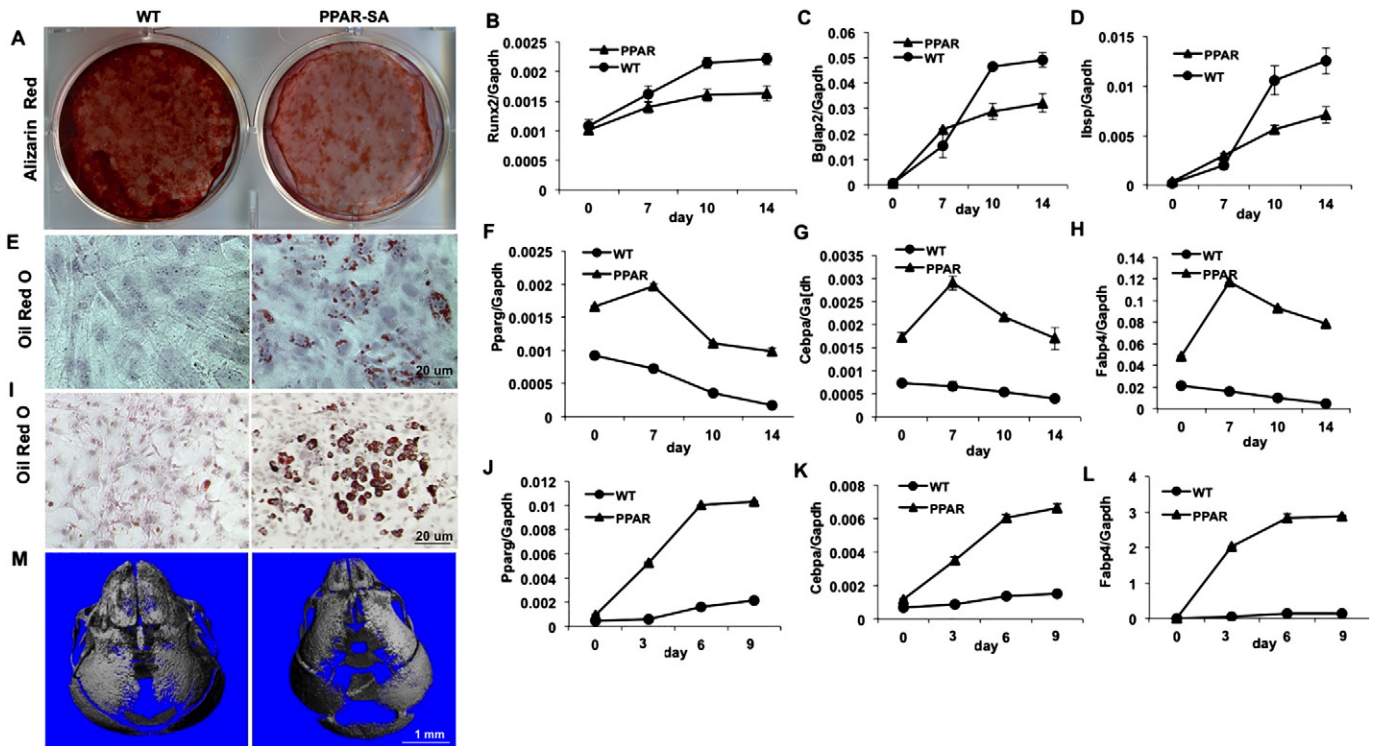


Fig. 5. Primary calvarial cultures from PPAR γ -S112A mice exhibit defective osteoblast differentiation and paradoxical increases in adipogenesis. (A–H) Growth of calvarial cells in osteogenic medium. Calvarial cells were prepared from male wild type and homozygous PPAR γ S112A mice and grown in osteoblast differentiation medium for the indicated times before measurement of osteoblast and adipocyte differentiation. (A–D) Osteoblast differentiation. Mineral deposition was measured by Alizarin red staining after 2 weeks (A). Total RNA was isolated at the times indicated for measurement of osteoblast marker mRNAs. (B) *Runx2* mRNA, (C) *Bglap2* mRNA and (D) *Ibsp* mRNA. (E–H) Adipocyte differentiation in osteogenic medium. Fat droplet accumulation (E) and adipocyte marker mRNAs (F–H) were measured in a parallel set of cultures also grown in osteogenic medium. Fat droplets were measured after 2 weeks using Oil red O staining. Adipocyte differentiation marker mRNAs were measured at the times indicated. (F) *Pparg*, (G) *Cebpa*, (H) *Fabp*. (I–L) Growth of calvarial cells in adipogenic medium. (I) Oil red O staining of primary calvaria cells grown in adipogenic conditions for 9 days. (J) *Pparg* mRNA, (K) *Cebpa* mRNA, (L) *Fabp* mRNA. (M) MicroCT scans of skulls from wild type and PPAR γ -S112A mice showing defective calvarial mineralization.

mutation on adipocyte/osteoblast differentiation by BMSCs must be considered. In fact, there is some precedent for peripheral fat having indirect effects on bone. For example, *PPAR γ ^{hyp/hyp}* mice contain a hypomorphic mutation in *Pparg* that causes a selective and dramatic reduction in *PPAR γ* levels in WAT without affecting spleen, bone, bone marrow or hematopoietic progenitors. These mice have very low peripheral fat and increased vertebral trabecular bone [36]. The observed increased bone mass was attributed to the reduced circulating leptin in these animals, which has been proposed to suppress bone formation through an indirect hypothalamic mechanism [37]. Paradoxically, leptin levels also decreased in *PPAR γ S112A* mice together with an increase in adiponectin (Fig. 2J, K), yet a low bone mass phenotype was observed, which is inconsistent with changes in bone and MAT being related to circulating leptin levels. Also, the observation that BMSCs from *PPAR γ S112A* mice preferentially differentiated to adipocytes at the expense of osteoblasts argues that effects of the *PPAR γ* mutation are cell autonomous and can occur in the absence of systemic, humoral signals.

A number of stimuli alter the osteoblast/adipocyte ratio in bone including skeletal loading, Wnt, PTH and FGF2 signaling [38–41]. Of these, mechanical loading is of particular interest. For example, exposure to low magnitude mechanical strain *in vivo* stimulates differentiation of MSCs to osteoblasts and decreases adipogenesis [38]. Also, biaxial mechanical strain or fluid shear loading of MSCs in cell culture inhibits adipocyte differentiation and stimulates osteoblast formation [42–44]. Conversely, *in vivo* skeletal unloading stimulates MAT formation while inhibiting bone formation *via* a *PPAR γ* -dependent pathway [45]. This is similar to the increased marrow adiposity and disuse osteopenia experienced by paraplegics [8]. Mechanical loading stimulates a broad range of signal transduction pathways including integrin-focal adhesion kinase, Wnt/ β -catenin, COX2 activation/PGE2 production and Rho/ROCK signaling. Interestingly, all these pathways directly or indirectly affect MAPK. For example, cell stretching or exposure to fluid flow shear stress activates integrin signaling followed by activation of focal adhesion kinase and MAPK [46]. Other loading-induced signals such as activation of Rho/ROCK and Wnt indirectly activate or are themselves activated by MAPK [47–49]. Thus, MAPK activation is a common loading-induced signal in bone with potential to stimulate differentiation of marrow cells to osteoblasts and away from adipocytes *via* phospho-regulation of RUNX2 and *PPAR γ* . Skeletal loading and unloading experiments will be required to determine the degree to which this pathway controls MAT and bone formation *in vivo*.

A final point for consideration is the relationship between the bone phenotype of *PPAR γ S112A* mice we report and previously characterized metabolic changes in these animals [27]. Similar to our results with BMSCs, MEFs from *PPAR γ S112A* mice show enhanced adipogenic differentiation in culture, but contrary to prediction, mice are not obese, but instead have normal amounts of WAT and BAT. While the number of adipocytes in peripheral fat from *PPAR γ S112A* mice is mildly increased, there is no net change in overall fat mass or distribution because cells are smaller. The *PPAR γ S112A* mutation also does not affect weight gain on normal or high fat diets, food intake or oxygen consumption. Interestingly, mutant mice are resistant to the negative effects of a high fat diet on insulin sensitivity and glucose tolerance and have reduced levels of free fatty acids and triglycerides. These metabolic changes may be related to the observed elevation in circulating adiponectin, which is known to increase insulin sensitivity and fatty acid oxidation [50]. As we recently showed, adiponectin secretion from MAT is greater than from WAT [5]. Furthermore, expansion of total MAT by caloric restriction or cancer therapy is associated with increased adiponectin. It is, therefore, possible that the observed elevation of adiponectin in *PPAR γ S112A* mice is at least in part caused by the expansion of MAT in these animals. If so, this would suggest that manipulation of MAT and bone by regulation of *PPAR γ* and RUNX2 phosphorylation as affected by mechanical loading or other signals is a potential way of controlling insulin sensitivity and systemic metabolism.

Disclosure

All authors state that they have no conflicts of interest.

Acknowledgements

This work was supported by NIH grants DE11723, a pilot grant from the Michigan Center for Diabetes Translational Research P30 DK092926 (RTF), DK092759, DK095705, DK62876 (OAM) and K12 DE023574 (Junior Faculty Training Award, CG). The authors thank Dr. Kenneth Kozloff (University of Michigan Medical School) for reviewing this manuscript.

Authors' roles

CG and RTF designed the research with assistance from WC and OM. CG, GZ, BL and YL conducted all experiments. RTF and CG wrote the manuscript. The manuscript was proofread and approved by all authors.

Appendix A. Supplementary data

Supplementary data to this article can be found online at <https://doi.org/10.1016/j.bone.2017.10.023>.

References

- [1] G. Karsenty, M. Ferron, The contribution of bone to whole-organism physiology, *Nature* 481 (7381) (2012) 314–320.
- [2] B. Lecka-Czernik, C.J. Rosen, Energy excess, glucose utilization, and skeletal remodeling: new insights, *J. Bone Miner. Res.* 30 (8) (2015) 1356–1361.
- [3] P.K. Fazeli, M.C. Horowitz, O.A. MacDougald, et al., Marrow fat and bone—new perspectives, *J. Clin. Endocrinol. Metab.* 98 (3) (2013) 935–945.
- [4] M.J. Devlin, A.M. Cloutier, N.A. Thomas, et al., Caloric restriction leads to high marrow adiposity and low bone mass in growing mice, *J. Bone Miner. Res.* 25 (9) (2010) 2078–2088.
- [5] W.P. Cawthorn, E.L. Scheller, B.S. Learman, et al., Bone marrow adipose tissue is an endocrine organ that contributes to increased circulating adiponectin during caloric restriction, *Cell Metab.* 20 (2) (2014) 368–375.
- [6] J. Justesen, K. Stenderup, E.N. Ebbesen, L. Mosekilde, T. Steiniche, M. Kassem, Adipocyte tissue volume in bone marrow is increased with aging and in patients with osteoporosis, *Biogerontology* 2 (3) (2001) 165–171.
- [7] P. Meunier, P. Courpron, C. Edouard, J. Bernard, J. Bringuier, G. Vignon, Physiological senile involution and pathological rarefaction of bone. Quantitative and comparative histological data, *Clin. Endocrinol. Metab.* 2 (2) (1973) 239–256.
- [8] P. Minaire, C. Edouard, M. Arlot, P.J. Meunier, Marrow changes in paraplegic patients, *Calcif. Tissue Int.* 36 (3) (1984) 338–340.
- [9] M.F. Pittenger, A.M. Mackay, S.C. Beck, et al., Multilineage potential of adult human mesenchymal stem cells, *Science* 284 (5411) (1999) 143–147.
- [10] P. Bianco, P. Gehron Robey, Marrow stromal stem cells, *J. Clin. Invest.* 105 (12) (2000) 1663–1668.
- [11] B.O. Zhou, R. Yue, M.M. Murphy, J.G. Peyer, S.J. Morrison, Leptin-receptor-expressing mesenchymal stromal cells represent the main source of bone formed by adult bone marrow, *Cell Stem Cell* 15 (2) (2014) 154–168.
- [12] T. Akune, S. Ohba, S. Kamekura, et al., *PPAR γ* insufficiency enhances osteogenesis through osteoblast formation from bone marrow progenitors, *J. Clin. Invest.* 113 (6) (2004) 846–855.
- [13] J. Bedore, K. Quesnel, D. Quinonez, C.A. Seguin, A. Leask, Targeting the annulus fibrosus of the intervertebral disc: Col1a2-Cre(ERT) mice show specific activity of Cre recombinase in the outer annulus fibrosus, *J. Cell Commun. Signal.* 10 (2) (2016) 137–142.
- [14] G. Xiao, R. Gopalakrishnan, D. Jiang, E. Reith, M.D. Benson, R.T. Franceschi, Bone morphogenetic proteins, extracellular matrix, and mitogen-activated protein kinase signaling pathways are required for osteoblast-specific gene expression and differentiation in MC3T3-E1 cells, *J. Bone Miner. Res.* 17 (1) (2002) 101–110.
- [15] G. Xiao, D. Wang, M.D. Benson, G. Karsenty, R.T. Franceschi, Role of the alpha2-integrin in osteoblast-specific gene expression and activation of the *Osf2* transcription factor, *J. Biol. Chem.* 273 (49) (1998) 32988–32994.
- [16] C.B. Khatiwala, P.D. Kim, S.R. Peyton, A.J. Putnam, ECM compliance regulates osteogenesis by influencing MAPK signaling downstream of RhoA and ROCK, *J. Bone Miner. Res.* 24 (5) (2009) 886–898.
- [17] J. You, G.C. Reilly, X. Zhen, et al., Osteopontin gene regulation by oscillatory fluid flow via intracellular calcium mobilization and activation of mitogen-activated protein kinase in MC3T3-E1 osteoblasts, *J. Biol. Chem.* 276 (16) (2001) 13365–13371.
- [18] Y. Li, C. Ge, J.P. Long, et al., Biomechanical stimulation of osteoblast gene expression requires phosphorylation of the RUNX2 transcription factor, *J. Bone Miner. Res.* 27 (2012) 1263–1274.
- [19] S. Kapur, S. Mohan, D.J. Baylink, K.H. Lau, Fluid shear stress synergizes with insulin-like growth factor-I (IGF-I) on osteoblast proliferation through integrin-dependent activation of IGF-I mitogenic signaling pathway, *J. Biol. Chem.* 280 (20) (2005) 20163–20170.

- [20] G. Xiao, D. Jiang, R. Gopalakrishnan, R.T. Franceschi, Fibroblast growth factor 2 induction of the osteocalcin gene requires MAPK activity and phosphorylation of the osteoblast transcription factor, Cbfa1/Runx2, *J. Biol. Chem.* 277 (39) (2002) 36181–36187.
- [21] G. Xiao, D. Jiang, P. Thomas, et al., MAPK pathways activate and phosphorylate the osteoblast-specific transcription factor, Cbfa1, *J. Biol. Chem.* 275 (6) (2000) 4453–4459.
- [22] C. Ge, G. Xiao, D. Jiang, et al., Identification and functional characterization of ERK/MAPK phosphorylation sites in the Runx2 transcription factor, *J. Biol. Chem.* 284 (47) (2009) 32533–32543.
- [23] C. Ge, G. Xiao, D. Jiang, R.T. Franceschi, Critical role of the extracellular signal-regulated kinase-MAPK pathway in osteoblast differentiation and skeletal development, *J. Cell Biol.* 176 (5) (2007) 709–718.
- [24] H.S. Camp, S.R. Tafuri, Regulation of peroxisome proliferator-activated receptor gamma activity by mitogen-activated protein kinase, *J. Biol. Chem.* 272 (16) (1997) 10811–10816.
- [25] E. Hu, J.B. Kim, P. Sarraf, B.M. Spiegelman, Inhibition of adipogenesis through MAP kinase-mediated phosphorylation of PPARgamma, *Science* 274 (5295) (1996) 2100–2103.
- [26] C. Ge, W.P. Cawthorn, Y. Li, G. Zhao, O.A. Macdougald, R.T. Franceschi, Reciprocal control of osteogenic and adipogenic differentiation by ERK/MAP kinase phosphorylation of Runx2 and PPARgamma transcription factors, *J. Cell. Physiol.* 231 (3) (2016) 587–596.
- [27] S.M. Rangwala, B. Rhoades, J.S. Shapiro, et al., Genetic modulation of PPARgamma phosphorylation regulates insulin sensitivity, *Dev. Cell* 5 (4) (2003) 657–663.
- [28] J.A. Fretz, T. Nelson, Y. Xi, D.J. Adams, C.J. Rosen, M.C. Horowitz, Altered metabolism and lipodystrophy in the early B-cell factor 1-deficient mouse, *Endocrinology* 151 (4) (2010) 1611–1621.
- [29] P. Ducy, G. Karsenty, Two distinct osteoblast-specific cis-acting elements control expression of a mouse osteocalcin gene, *Mol. Cell. Biol.* 15 (4) (1995) 1858–1869.
- [30] P.H. Krebsbach, M.H. Mankani, K. Satomura, S.A. Kuznetsov, P.G. Robey, Repair of craniotomy defects using bone marrow stromal cells, *Transplantation* 66 (10) (1998) 1272–1278.
- [31] E.J. Moerman, K. Teng, D.A. Lipschitz, B. Lecka-Czernik, Aging activates adipogenic and suppresses osteogenic programs in mesenchymal marrow stroma/stem cells: the role of PPAR-gamma2 transcription factor and TGF-beta/BMP signaling pathways, *Aging Cell* 3 (6) (2004) 379–389.
- [32] C. Ge, Z. Wang, G. Zhao, et al., Discoidin receptor 2 controls bone formation and marrow adipogenesis, *J. Bone Miner. Res.* 31 (12) (2016) 2193–2203.
- [33] C. Ge, Q. Yang, G. Zhao, H. Yu, K.L. Kirkwood, R.T. Franceschi, Interactions between extracellular signal-regulated kinase 1/2 and p38 MAP kinase pathways in the control of RUNX2 phosphorylation and transcriptional activity, *J. Bone Miner. Res.* 27 (3) (2012) 538–551.
- [34] Y. Wan, L.W. Chong, R.M. Evans, PPAR-gamma regulates osteoclastogenesis in mice, *Nat. Med.* 13 (12) (2007) 1496–1503.
- [35] L.A. Stechschulte, C. Ge, T.D. Hinds Jr., E.R. Sanchez, R.T. Franceschi, B. Lecka-Czernik, Protein phosphatase PP5 controls bone mass and the negative effects of rosiglitazone on bone through reciprocal regulation of PPARgamma (peroxisome proliferator-activated receptor gamma) and RUNX2 (runt-related transcription factor 2), *J. Biol. Chem.* 291 (47) (2016) 24475–24486.
- [36] T.A. Cock, J. Back, F. Elefteriou, et al., Enhanced bone formation in lipodystrophic PPARgamma(hyp/hyp) mice relocates haematopoiesis to the spleen, *EMBO Rep.* 5 (10) (2004) 1007–1012.
- [37] P. Ducy, M. Amling, S. Takeda, et al., Leptin inhibits bone formation through a hypothalamic relay: a central control of bone mass, *Cell* 100 (2) (2000) 197–207.
- [38] Y.K. Luu, E. Capilla, C.J. Rosen, et al., Mechanical stimulation of mesenchymal stem cell proliferation and differentiation promotes osteogenesis while preventing dietary-induced obesity, *J. Bone Miner. Res.* 24 (1) (2009) 50–61.
- [39] W.P. Cawthorn, A.J. Bree, Y. Yao, et al., Wnt6, Wnt10a and Wnt10b inhibit adipogenesis and stimulate osteoblastogenesis through a beta-catenin-dependent mechanism, *Bone* 50 (2) (2012) 477–489.
- [40] L. Xiao, T. Sobue, A. Eslinger, et al., Disruption of the Fgf2 gene activates the adipogenic and suppresses the osteogenic program in mesenchymal marrow stromal stem cells, *Bone* 47 (2) (2010) 360–370.
- [41] Y. Fan, J.I. Hanai, P.T. Le, et al., Parathyroid hormone directs bone marrow mesenchymal cell fate, *Cell Metab.* 25 (3) (2017) 661–672.
- [42] V. David, A. Martin, M.H. Lafage-Proust, et al., Mechanical loading down-regulates peroxisome proliferator-activated receptor gamma in bone marrow stromal cells and favors osteoblastogenesis at the expense of adipogenesis, *Endocrinology* 148 (5) (2007) 2553–2562.
- [43] B. Sen, Z. Xie, N. Case, M. Ma, C. Rubin, J. Rubin, Mechanical strain inhibits adipogenesis in mesenchymal stem cells by stimulating a durable beta-catenin signal, *Endocrinology* 149 (12) (2008) 6065–6075.
- [44] Y. Tanabe, M. Koga, M. Saito, Y. Matsunaga, K. Nakayama, Inhibition of adipocyte differentiation by mechanical stretching through ERK-mediated downregulation of PPARgamma2, *J. Cell Sci.* 117 (Pt 16) (2004) 3605–3614.
- [45] P.J. Marie, K.P.P.A.R. Kaabeche, Gamma activity and control of bone mass in skeletal unloading, *PPAR Res.* 2006 (2006) 64807.
- [46] S.R. Young, R. Gerard-O'Riley, J.B. Kim, F.M. Pavalko, Focal adhesion kinase is important for fluid shear stress-induced mechanotransduction in osteoblasts, *J. Bone Miner. Res.* 24 (3) (2009) 411–424.
- [47] I. Cervenka, J. Wolf, J. Masek, et al., Mitogen-activated protein kinases promote WNT/beta-catenin signaling via phosphorylation of LRP6, *Mol. Cell. Biol.* 31 (1) (2011) 179–189.
- [48] E.C. Lessey, C. Guilly, K. Burridge, From mechanical force to RhoA activation, *Biochemistry* 51 (38) (2012) 7420–7432.
- [49] A.G. Robling, The expanding role of Wnt signaling in bone metabolism, *Bone* 55 (1) (2013) 256–257.
- [50] R. Ye, P.E. Scherer, Adiponectin, driver or passenger on the road to insulin sensitivity? *Mol. Metab.* 2 (3) (2013) 133–141.